# Sensitivity Analysis of Suspension Parameters of the Critical Velocity of a Railway Bogie on a Tangent Track Using Standardized Regression Coefficients

Thanaporn Talingthaisong[1] Sedthawatt Sucharitpwatskul[2] Anchalee Manonukul[3]
Panya Kansuwan[4*]

[1,2,3]*National Metal and Materials Technology Center,*
*National Science and Technology Development Agency (NSTDA), Pathum Thani, Thailand*
[4*]*Department of Mechanical Engineering, School of Engineering,*
*King Mongkut's Institute of Technology Ladkrabang, Bangkok, Thailand*

*Corresponding Author. E-mail address: panya.ka@kmitl.ac.th

Received: 26 November 2022; Revised: 1 March 2023; Accepted: 28 April 2023
Published online: 29 June 2023

***Abstract***

This paper presents the sensitivity analysis using standardized regression coefficients (SRC) to enumerate an important factor of each suspension parameter on the critical velocity of a bogie. Due to uncertain parameters, the semi-global sensitivity analysis benefits both designers and maintenance engineers in controlling the risk levels of the screened components. The bogie represents a two-axle railway truck of the State Railway of Thailand (SRT). Six-degree-of-freedom motion equations describe its dynamic behaviors traveling on a tangent track. In a stochastic model, the stiffness and damping coefficients of suspension components are considered random variables with presumed Gaussian distribution. A probability distribution obtained, where the SRCs were derived, shows that the speed strongly correlates with the longitudinal yaw stiffness value of the primary suspension system. The secondary suspension system's lateral and longitudinal yaw damping coefficients appear equally influential on the critical speed.

***Keywords*:** Monte Carlo method, Probability safety assessment, Railway bogie, Reliability analysis, Vehicle dynamics

## I. INTRODUCTION

Recently, the railway industry has faced the challenges of reducing manufacturing costs while maintaining marginal engineering safety. Operators first provide conceptual requirements to engineering teams to design the vehicles with constructed infrastructures expected to be in service for predefined service life against relevant damage mechanisms. After the vehicle is fabricated, it must pass safety requirements according to applicable railway safety standards. However, critical items deteriorate at different rates, and the defects that occur further degrade operating performance. Monitoring the key performance indicators can help maintenance engineers identify the parts to be inspected and keep the damage within a safe range. This defect-tolerance design strategy partly leaves the safety issues to maintenance departments to inspect based on time or risk measurements. In either method, knowledge management along the engineering design process on the sensitive parts is inevitable. To ensure safe operation, railway engineers must understand the rank of the influential parameters of the railway vehicles on the critical speed to set railway operating windows of the vehicles. Overlooking the life-critical components may lead to a severe accident that could cost human lives.

A railway system's safe and economic operation depends on the railway vehicles' running performance in service. The acceptable conditions of the vehicles are described in EN14363 [1] and UIC 518 [2]. One of the safety issues is the safety against derailment as quantified by a limiting ratio of the lateral to vertical forces at a flange contact due to lateral oscillation motion. The hunting motion, arising from non-conservative forces, causes vehicle instability beyond a critical velocity. The further the operation speed, the more violent the oscillation and eventually causes severe flange wear, wheel climbing, and derailment.

Since stability is essential to the safe operation of railway vehicles, the oscillation motion on tangent tracks has been the subject of intense investigations using four, six, or ten degrees of freedom models. Wheelsets' lateral displacement and yaw angle are the state variables in 4-DOF systems [3]-[7]. When the bogie's lateral displacement and yaw angle are considered, the 6-DOF models were investigated in different aspects [8]–[13]. Up to 10 DOF systems consider more on each wheelset's vertical and roll angle [14], [15]. The works relied on linearizing a system of governing differential equations to study the bogie's dynamic behaviors traveling on a straight track. In particular, the suspension parameters and wheel conicity are two categories of parameters in consideration. Wickens [6] showed that a model required at least 6-DOF for realistic stability analysis. Flexibility between the wheelset and the frame and wheel/rail profile should be considered in the design of high-speed railway vehicles. More flexible damped or stiffer suspension is preferable [10], [11]. The effect of nonlinear yaw dampers on the behavior was studied by Mehdi and Shaopu [10] using the Bogoliubov averaging method. A local sensitivity, as a result, suggests the influence of the secondary suspension parameters. Due to existing nonlinear creep forces at the interface, two-axle trucks indicate subcritical Hopf bifurcation dynamic behaviors [3], [5], [8], [16], [17]. They found that the critical velocity on a tangent track strongly depended on characteristics of the wheel/rail interface expressed as conicity.

A central point of the present study is to determine the critical velocity and the sensitivity of each parameter on the velocity of a railway bogie of SRT. The physical parameters of primary and secondary suspension, including conicity, are provided with a predetermined probability distribution. The sensitivity analysis method is a hybrid local-global scheme on the

linearized model. The Monte Carlo method [18] is implemented to generate the parameters as random variables to be distributed normally about their specific operative means with a standard deviation of 10% of the means. The condition for critical velocity data acquirement is when the real part of each root of the characteristic equation derived from the six-DOF bogie truck system is recognized as positive at which the bifurcation points are located. The distribution of the obtained critical velocity is assessed as an influence measure by the normalized factor's standard deviation compared to those influenced by other parameters. Classification of these parameters benefits designers and service engineers in discriminating between critical and less critical parameters. Delaying damage mechanisms that compromise the elements relevant to the vital parameters will then prolong the safe operating lifetime of the system. Keeping the part fitted in service with a risk-based maintenance strategy needs a quick calculation of the sensitivity of the parameters. Less distributed measurements of the parameter can mitigate risk. The standardized regression coefficients (SRC) conducted is the method that includes both the effect of physical behavior and the uncertainty of the measured parameters.

## II. METHODOLOGY

### *A. Equations of Motion of a Wheelset on a Tangent Track*

A wheelset is a crucial component that governs the dynamic behaviors of railway vehicles. This study employs wheelset motion equations based on an equilibrium track coordinate system to specify a bogie mathematical model [10], [14]. The wheelset dynamic equation describes the system when the bogie travels on a tangent track at a constant speed. Figure 1 illustrates the free-body diagram of the wheelset in which $F_{ix}$ and $F_{iy}$ are creep forces in the longitudinal and lateral direction on the left ($i = L$) and right ($i = R$) wheel/rail contact points. $M_{iz}$ is the creep moments about the vertical direction Equations for lateral and vertical motions in the equilibrium axes derived from Newton's law are:

$$m\ddot{y} = F_{Ly} + F_{Ry} + N_{Ry} + N_{Ly} + F_{sy} - F_T \tag{1}$$

$$m\ddot{z} = F_{Lz} + F_{Rz} + N_{Rz} + N_{Lz} + F_{sz} - W_A \tag{2}$$

$$\begin{aligned} I_x\ddot{\phi} - (I_y - I_z)\dot{\theta}\,\dot{\psi} = {} & R_{Ry}(F_{Rz} + N_{Rz}) \\ & -R_{Rz}(F_{Ry} + N_{Ry}) + R_{Ly}(F_{Lz} + N_{Lz}) \\ & -R_{Lz}(F_{Ly} + N_{Ly}) \end{aligned} \tag{3}$$

$$\begin{aligned} I_z\ddot{\psi} - (I_{wx} - I_{wy})\dot{\phi}\,\dot{\theta} = {} & R_{Rx}(F_{Ry} + N_{Ry}) - R_{Ry}F_{Rx} \\ & + R_{Lx}(F_{Ly} + N_{Ly}) - R_{Ly}F_{Lx} \\ & + M_{Lz} + M_{Rz} + M_{sz} \end{aligned} \tag{4}$$

in which $\vec{N}_L = N_L cos(\delta_L + \phi)\hat{\imath} + N_L sin(\delta_L + \phi)\hat{\jmath}$, $\vec{N}_R = N_R cos(\delta_R - \phi)\hat{\imath} - N_R sin(\delta_R - \phi)\hat{\jmath}$. $N_i$ is the normal contact force and $\delta_i$ is contact angle. $\phi$ and $\psi$ are roll angle and yaw angle, respectively.

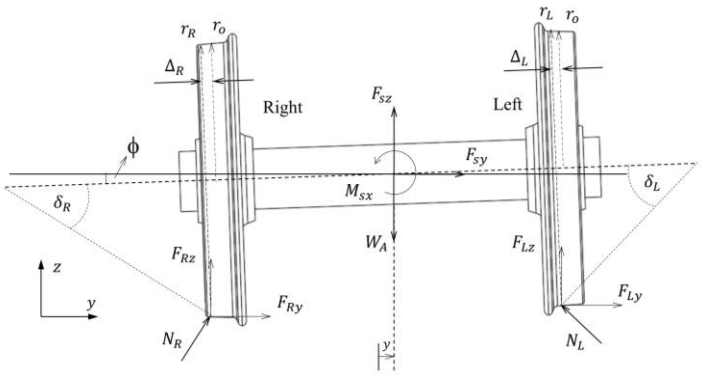


Figure 1: The free-body diagram of a wheelset

For small perturbation from the wheelset's equilibrium position, the magnitude of normal contact forces are

$$N_L cos(\delta_L + \phi) \approx \frac{1}{2}(W_A - F_{sz}) - (2a)^{-1}(r_R F_{Ry} + r_L F_{Ly}) \quad (5)$$

$$N_R cos(\delta_R - \phi) \approx \frac{1}{2}(W_A - F_{sz}) + (2a)^{-1}(r_R F_{Ry} + r_L F_{Ly}) \quad (6)$$

According to Kalker's linear creep theory, creep forces as functions of creepages are:

Longitudinal creep force:

$$F_x = -f_{33}\boldsymbol{\xi}_x \quad (7)$$

Lateral creep force:

$$F_y = -f_{11}\xi_y - f_{12}\xi_{sp} \quad (8)$$

Spin creep moment:

$$M_z = f_{12}\xi_y - f_{22}\xi_{sp} \quad (9)$$

in which $\xi_x, \xi_y, \xi_{sp}$ are longitudinal, lateral, and spin creepages in Table 1 [14]. $f_x, f_y, f_{sp}$ are creep coefficients as provided in [10].

The determination of the lateral suspension forces and the vertical suspension moment are presented in Eq. (10). Moreover, Eq. (11) applied to the 6-DOF model (Figure 2) in terms of lateral and longitudinal stiffness ($K_w$) and damp coefficient ($C_w$).

Longitudinal creep force:

$$F_{s,y} = -2K_{wy}y - 2C_{wy}\dot{y} \quad (10)$$

Vertical suspension moment:

$$M_{s,z} = -2K_{wx}b_1^2 - 2C_{wx}b_2^2 \quad (11)$$

Table 1: Creepage at the Left/Right Wheel/Rail Contact Points [14]

| **Left Wheel/Rail Contact Point** |
|---|
| $\xi_{xL} = \frac{1}{V}\left(V - \frac{r_L}{r_o} - a\dot{\psi}\right)$ |
| $\xi_{yL} = \frac{1}{V}(\dot{y} + r_L\dot{\phi} - V\psi)cos(\delta_L + \phi)$ |
| $\xi_{spL} = \frac{1}{V}\{\dot{\psi}cos(\delta_L + \phi) - \Omega sin(\delta_L)\}$ |
| **Right Wheel/Rail Contact Point** |
| $\xi_{xR} = \frac{1}{V}\left(V - \frac{r_R}{r_o} + a\dot{\psi}\right)$ |
| $\xi_{yR} = \frac{1}{V}(\dot{y} + r_R\dot{\phi} - V\psi)cos(\delta_L - \phi)$ |
| $\xi_{spR} = \frac{1}{V}\{\dot{\psi}cos(\delta_R - \phi) + \Omega sin(\delta_R)\}$ |

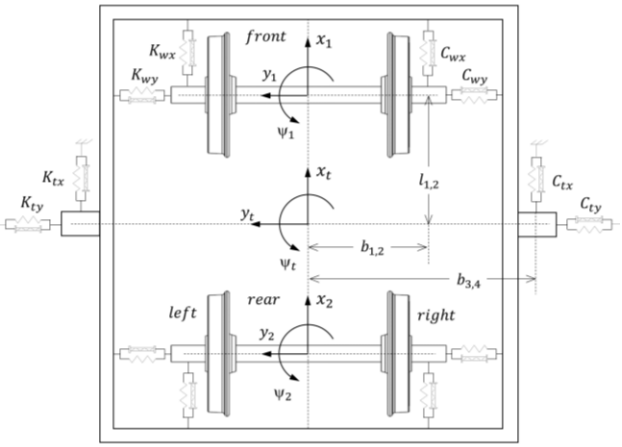


Figure 2: Two-axle bogie configuration

To prevent derailment of the vehicle operating at a velocity higher than a critical speed, a nonlinear flange contact force is

$$F_T = \begin{cases} K_r(y - \delta) & y > \delta \\ 0 & -\delta \le y \le \delta \\ K_r(y + \delta) & y < -\delta \end{cases} \quad (12)$$

in which $K_r$ is the wheel/rail contact lateral stiffness. $\delta$ is the flange clearance determined when the first abrupt change of rolling radius difference values occurs, as indicated in Figure 3, using the semi-analytical method [1]. The wheelset is shifted laterally to create a contact locus to determine a yaw-angle that satisfies the criteria of an equi-vertical distance between each pair of left/right wheel and rail profiles. The wheel profile is Vidura provided by SRT, while the 54E1 rail profile refers to EN13674-1 [2].


Figure 3: Determination of flange clearance

By substituting Eq. (5) and (6) into Eq. (1) and Eq. (4) for normal contact force, the motion equations of the wheelset become Eq. (13) and Eq. (14), respectively, when further using Eq. (15) and neglecting high-order terms.

$$m_w\ddot{y} + \frac{2f_{11}}{V}\left(\dot{y} + \frac{r_L+r_R}{2}\dot{\phi} - V\psi\right) + 2f_{33}\psi\left(1 - \frac{r_L+r_R}{2R_o}\right) + 2f_{12}\left(\frac{\dot{\psi}}{V} - \frac{\delta_L-\delta_R}{2R_o}\right) + m_w g\left(\frac{\delta_L-\delta_R}{2} + \phi\right) = F_{s,y} - F_T \quad (13)$$

$$I_{wz}\ddot{\psi} + \left(I_{wy} - I_{wx}\right)\frac{V}{R_o}\dot{\phi} + \frac{2af_{33}}{R_o}\frac{r_L-r_R}{2} - \frac{2f_{12}}{V}\left(\dot{y} + \frac{r_L+r_R}{2}\dot{\phi} - V\psi\right) + \frac{2a^2f_{33}}{V}\dot{\psi} - 2f_{22}\frac{\delta_L-\delta_R}{2R_o} - am_w g\frac{\delta_L+\delta_R}{2}\psi + \frac{2f_{22}}{V}\dot{\psi} = M_{s,z} \quad (14)$$

$$\delta_L = \delta_R = \lambda, \frac{1}{2}(r_L - r_R) = \lambda y, \frac{1}{2}(r_L + r_R) = r_0, \phi = \lambda\frac{y}{d} \quad (15)$$

The linearized differential equations of wheelsets when $i = 1$ represents the front axle and $i = 2$ represents the rear axle are Eq. (16) and (17).

$$m_w\ddot{y}_i + \frac{2f_{11}}{V}\left[\left(1 + r_o\frac{\lambda}{d}\right)\dot{y}_i - V\psi_i\right] + \frac{2f_{12}}{V}\dot{\psi}_i + W_A\frac{\lambda}{d}y_i = F_{s,yi} - F_{Ti} \quad (16)$$

$$-\frac{2f_{12}}{V}\left[\left(1 + r_o\frac{\lambda}{a}\right)\dot{y}_i - V\psi_i\right] + \frac{2d^2f_{33}}{V}\dot{\psi}_i - aW_A\lambda\psi_i + \frac{2f_{12}}{V}\dot{\psi}_i = M_{s,zi} \quad (17)$$

The governing differential equations of the motion of the bogie frame for lateral and yaw movement are

$$m_t\ddot{y}_t = -F_{sy1} - F_{sy2} - 2K_{ty}y_t - 2C_{ty}\dot{y}_t \quad (18)$$

$$\begin{aligned} I_{wz}\ddot{\psi}_t = {} & -2K_{wy}\left[y_1 - y_t + l_1\psi_t\right]l_1 \\ & +2K_{wy}\left[y_2 - y_t - l_1\psi_t\right]l_1 \\ & -2C_{wy}\left[\dot{y}_1 - \dot{y}_t + l_2\dot{\psi}_t\right]l_2 \\ & +2C_{wy}\left[\dot{y}_2 - \dot{y}_t - l_2\dot{\psi}_t\right]l_2 \\ & -2K_{tx}b_3^2\psi_t - 2C_{tx}b_4^2\dot{\psi}_t \\ & +2K_{wx}b_1^2\left(\psi_1 + \psi_2 - 2\psi_t\right) \\ & +2C_{wx}b_2^2\left(\psi_1 + \psi_2 - 2\dot{\psi}_t\right) \end{aligned} \quad (19)$$

Eq. (16)-(19) complete the 6-DOF system of motion for the two-axle bogie on a straight track considered in this paper. Table 2 provides the nomenclatures and operative values of system parameters.

Table 2: Nomenclature and system parameters used for numerical analysis [10]

| Parameter | Symbol | [10] | SRT | Unit |
|---|---|---|---|---|
| Half of the track gauge | $a$ | 0.7176 | 0.5000 | $m$ |
| Lateral rail stiffness | $K_r$ | 1.617E7 | 1.617E7 | $N/m$ |
| Flange clearance | $\delta$ | 0.00923 | 0.00740 | $m$ |
| Wheel radius | $r_o$ | 0.5330 | 0.4255 | $m$ |
| Wheel conicity | $\lambda$ | 0.0500 | 0.0536 | - |
| Wheelset mass | $m_w$ | 1800 | 1542 | $kg$ |
| Moment of inertia of the wheelset – roll component | $I_{wx}$ | 625.7 | 272.2 | $kg \cdot m^2$ |
| Moment of inertia of the wheelset – pitch component | $I_{wy}$ | 133.90 | 73.15 | $kg \cdot m^2$ |
| Moment of inertia of the wheelset – yaw component | $I_{wz}$ | 625.7 | 272.2 | $kg \cdot m^2$ |
| Total bogie mass | $m$ | - | 5500 | $kg$ |
| Axle load | $W_A$ | 38492 | 42620 | $N$ |
| Mass of bogie frame | $m_t$ | 4255.6 | 2439.0 | $kg$ |
| Moment of inertia of bogie frame in yaw | $I_{tz}$ | 10314 | 1998 | $kg \cdot m^2$ |
| Primary suspension - Lateral stiffness | $K_{wy}$ | 8.67E4 | 1.87E5 | $N/m$ |
| Primary suspension - Lateral damping coefficient | $C_{wy}$ | 2.10E4 | - | $N \cdot s/m$ |
| Primary suspension – Longitudinal yaw spring stiffness | $K_{wx}$ | 8.67E4 | 1.87E5 | $N/m$ |
| Primary suspension - Longitudinal yaw damping coefficient | $C_{wx}$ | 1.92E4 | - | $N \cdot s/m$ |
| Secondary suspension - Lateral stiffness | $K_{ty}$ | 1.532E5 | 8.0E5 | $N/m$ |
| Secondary suspension - Lateral damping coefficient | $C_{ty}$ | 5.254E4 | 2.5E4 | $N \cdot s/m$ |
| Secondary suspension - Longitudinal yaw spring stiffness | $K_{tx}$ | 2.189E5 | 8.0E5 | $N/m$ |
| Secondary suspension - Longitudinal yaw damping coefficient | $C_{tx}$ | 6.129E5 | 2.5E5 | $N \cdot s/m$ |
| Half of the primary longitudinal yaw spring arm | $b_1$ | 1.0000 | 0.7875 | $m$ |
| Half of the primary longitudinal yaw damper arm | $b_2$ | 1.2700 | 0.7875 | $m$ |
| Half of the secondary longitudinal yaw spring arm | $b_3$ | 0.7940 | 0.7875 | $m$ |
| Half of the secondary longitudinal yaw damper arm | $b_4$ | 0.889 | 1.095 | $m$ |
| Half of the longitudinal distance of the lateral secondary spring | $l_1$ | 1.295 | 1.15 | $m$ |
| Half of the longitudinal distance of the lateral secondary dampers | $l_2$ | 1.295 | 1.15 | $m$ |

*B. Sensitivity Analysis Using Standardized Regression Coefficient (SRC) [3]*

Sensitivity analysis is typically implemented to assess model input factor's relative importance. To the first intuition, sensitivity can be evaluated by computing partial derivatives of an output variable concerning other dependent parameters. A parameter giving a higher value of the derivative shows more the extent of output change per unit change of the input when other variables are constant. The principle represents local sensitivity that is independent of the factor's uncertainty. The sensitivity analysis can be performed in a deterministic or probabilistic way. A type of sensitivity analysis performed in the context of stochastic analysis provides information regarding the distribution of random variables. A better measure for such an analysis is considering the factor's standard deviation according to Eq. (20). Due to the calculation, assumptions must be made about the range of variation of the element; thus, Eq. (20) is a hybrid local-global measure.

$$S_x^y = \frac{\sigma_x}{\sigma_y}\frac{\partial y}{\partial x} \tag{20}$$

where $S_x^y$ is the sensitivity of output $y$ to the factor parameter $x$, $\sigma_j$ is the standard deviation of the parameter. The suspension parameters of interest are those mentioned in the last sections. To express their sensitivity to critical velocity, we assume a normal distribution of each parameter with a standard deviation of 10% of its operating design value. Also, to consider the influence of uncertainty, the standard deviation of $K_{wx}$ varies at 5%, 10% and 20%. Normally, Eq. (20) is commonly not used for sensitivity analysis because the coefficients, $\frac{\partial y}{\partial x}$, are dimensioned. As a result, the practice is to compute the standardized regression coefficients, SRC ($\beta_x$), defined in a regression model as:

$$\tilde{y} = \frac{y - \bar{y}}{\sigma_y} = \beta_x \frac{x - \bar{x}}{\sigma_x}; \tag{21}$$

in which $\tilde{y}$ is the vector of regression model prediction. Eq. (21) insinuates that $\beta_x = S_x^y$ under the linear model assumption.

## III. RESULTS AND DISCUSSION

*A. Numerical Analysis of the Critical Speed of the Two-axle Bogie*

We solved the eigenvalue problems numerically to determine the critical velocity of the bogie. The state-space equations of the motion are transformed in the form of Eq. (22)–(23) below

$$\dot{X} = A(V)X + F(X) \tag{22}$$

in which $A(V)X$ represents the linear term and $F(X)$ represent the nonlinear term. $X(t)$ is a 12-column matrix of state variables describing the lateral and yaw motion of the wheelsets and bogie frame.

$$X = \{y_1, \dot{y}_1, \psi_1, \dot{\psi}_1, y_2, \dot{y}_2, \psi_2, \dot{\psi}_2, y_t, \dot{y}_t, \psi_t, \dot{\psi}_t\}^t \tag{23}$$

At different velocities, an eigenvalue and eigenvector problem of $A(V)$ is solved repeatedly. The system becomes unstable when at least one resolved eigenvalue is a positive real number. However, it is undetermined when a pair of the eigenvalues is imaginary. Consequently, the critical velocity ($V_c$) is the highest velocity at which all the eigenvalues associated with the matrix are negative real numbers. The numerical method results in Figure 4, in which the dot marker represents the critical velocity at 43.3 m/s with the contact conicity of 0.0536. The conicity was calculated from the contact pair profile configuration of the Vidura wheel profile and 54E1 rail profile. When using the same parameters presented by Mehdi and Shaopu [4], we obtain the same critical velocity of the bogie is 32.8 m/s at a conicity of 0.05.

For demonstrating the hunting phenomena of the vehicle, Eq. (16)–(19) are solved numerically using the

4th order Runge-Kutta integration scheme [5]. Lateral displacements of each wheelset ($y_1, y_2$) and of the truck ($y_t$) oscillating with time are presented in Figure 5a) at the velocity of 40 m/s located in undamped regime and in Figure 5b) at the velocity of 45 m/s located on the other side. Initial lateral displacement of the front wheelset ($y_1$) is set to be 5 mm, while all other initial values are zeros.

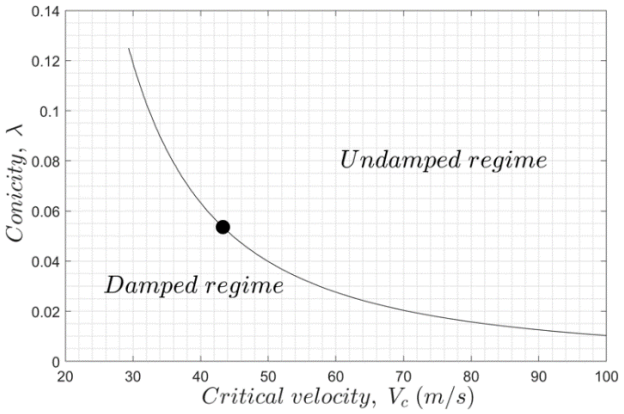


Figure 4: Numerical calculation of $V_c$ versus $\lambda$

At velocities less than $V_c$, the amplitudes of lateral displacements asymptotically vanish in the absence of track irregularity. The dynamic behavior is an underdamped system where the magnitude of the negative real part of system eigenvalues specifies the decay rate. Upon increasing the velocities above $V_c$, the vehicle vibrates as an undamped system but is limited by the wheel flange constraint with the rail. The amplitude of wheelset displacement is greater than 7.4 mm possessing a risk of a flange climb. Preventing a flange climb that leads to derailment is paramount for safe operations. Consequently, a derailment ratio is denoted as $Y/Q$ in which $Y$ and $Q$ are the lateral and vertical forces in the flange contact, respectively. According to Nadal's theory in UIC 518 regulation, $Y/Q$ is limited to 0.8 when the flange angle is 65° when using the coefficient of friction of 0.5.

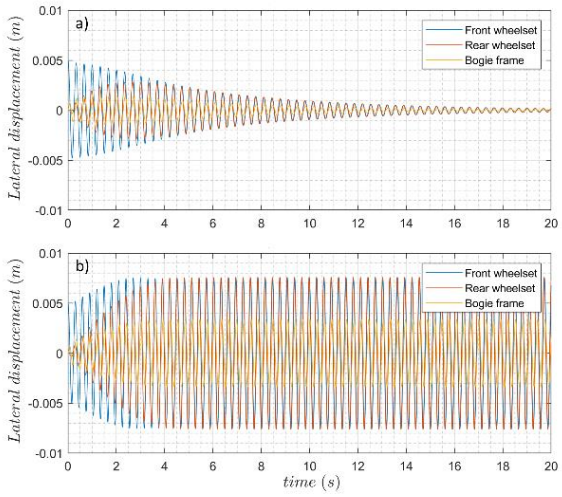


Figure 5: Time response of lateral displacement
a) 40 m/s b) 45 m/s

*B. The Relationship of Each Suspension System Parameter on the Critical Velocity*

Suspension systems of the two-axle bogie usually consist of two-stage primary and secondary suspension. The main components are springs and dampers arranged to secure a stable running behavior and safety. Springs and dampers between the bogie frame and the wheelset are of primary suspension. The lateral motion of the wheelset is controlled by two pairs of springs and dampers on both sides. The other two pairs, oriented in a longitudinal direction, assist in securing the yaw motion of the wheelset. The car body is connected to the bogie via the secondary suspension system, in which two pairs of springs and dampers orient in the lateral and longitudinal directions.

Figure 6 exhibits stability diagrams for spring stiffness and the damping coefficient of springs and dampers in the primary suspension. Two regions separated by the resulting curves are typically recognized. When operating in the left region of the curve, the vehicle is in subcritical bifurcation phenomena with vanishing displacement amplitude with time. However, when operating in the right area, the vehicle exhibits supercritical Hopf

bifurcation and oscillates till constrained by flange contact forces. $K_{wy}$ and $K_{wx}$ increase with the critical velocity about the operating stiffness. If the spring stiffness is greater than 4.5E5 N/m, the critical velocity decreases with increasing $K_{wy}$. It should be noted that our range of consideration may be unrealistically wide but just for an intuitive point. For comparison, each figure has a filled dot representing the operating physical parameter (Table 2) and its corresponding critical velocity.

Figure 7 demonstrates the monotonic relationship of the secondary suspension parameters with critical velocity. Increasing $K_{ty}, C_{ty}, K_{tx}, C_{tx}$ increases the critical velocity. However, the correlations become obscure in the comparative aspects of the parameters.

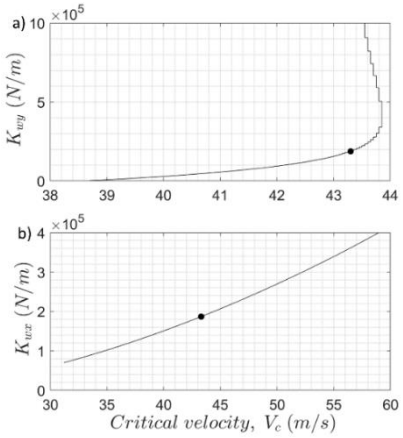


Figure 6: The effect of primary suspension parameters on limited speed

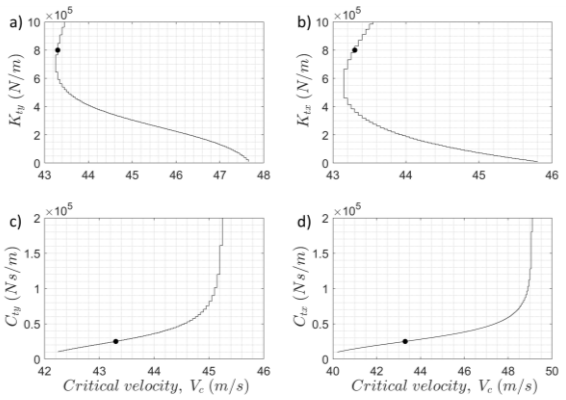


Figure 7: The effect of secondary suspension parameters on limited speed

*C. Sensitivity Analysis of Two-axle Bogie's Stability*

To classify the relative importance, we perform a Monte Carlo experiment on the model for sensitivity analysis to create scatter plots of the normalized critical velocity versus normalized physical parameters of each component in Figure 8–Figure 10. The model parameters are generated in a column matrix for 10000 data sets according to their distribution before being substituted into the mathematical model to compute critical velocity. The number of data sets is large enough to provide meaningful statistical results without too much loading on our computational resources. The normal distribution of calculated critical velocity obtained after substituting the random parameter matrix into the dynamic model is shown in Figure 11. Averaged critical velocity is 43.44 m/s with a standard deviation of 2.28.

$\tilde{K}_{wx}$ is recognized immediately in Figure 8a as the most influential factor when compared to $\tilde{K}_{wy}$ in Figure 8b and $\tilde{K}_{ty}, \tilde{C}_{ty}, \tilde{K}_{tx}, \tilde{C}_{tx}$ in Figure 9. The aggregated data in circular-like bounded shapes on the x-y plane characterize weak correlations in contrast to the case in which the scattered data are bound in the tilted band. Nevertheless, the local dependency of $K_{wy}$ in Figure 6b and $K_{ty}, C_{ty}, K_{tx}, C_{tx}$ in Figure 7 are smeared out due to the variation of the measured data. The other strong influence similar to $\tilde{K}_{wx}$ is also observed for the conicity in Figure 10, but in negative correlation, i.e., the increase of the conicity reduces the critical velocity. This qualitative recognition is invaluable for understanding the system but hard to be implemented as an input to commercial probability safety assessment programs if numeric values are required. When the quantitative sense is necessary, the stiffness value should be paid to control vehicle safety and performance. The important factor of both primary and secondary suspension elements, including conicity, are

determined quantitatively using the linear regression method of the distributed data according to Eq. (20).

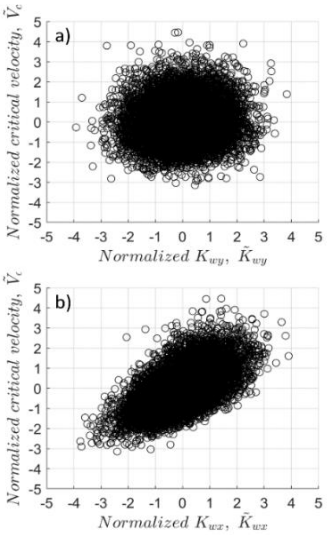


Figure 8: Scatter plot of $\tilde{y}$ versus $\tilde{V}_c$ using $\sigma_x = 10\%$

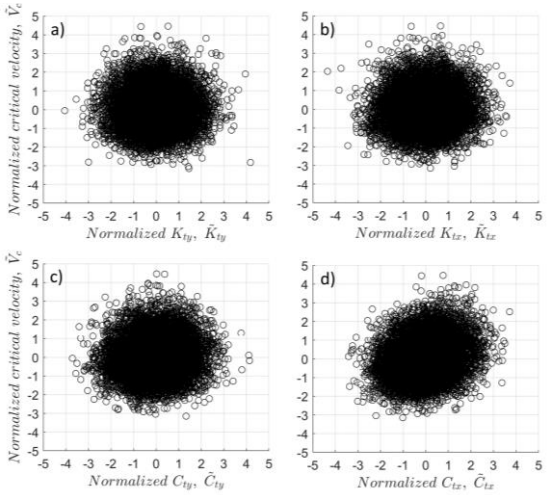


Figure 9: Scatter plot of $\tilde{y}$ versus $\tilde{V}_c$ using $\sigma_x = 10\%$

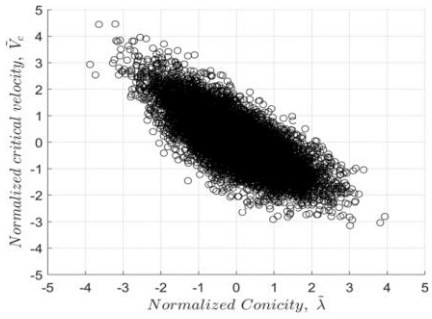


Figure 10: Scatter plots for $\tilde{\lambda}$ versus $\tilde{V}_c$ using $\sigma_x = 10\%$

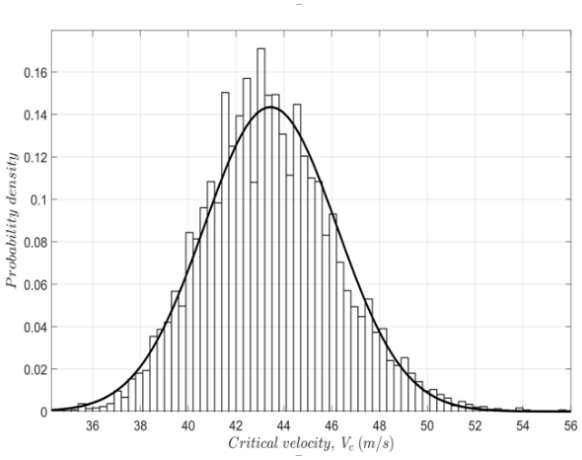


Figure 11: Output distribution from a Monte Carlo simulation of 10000 experiments, employing nine input parameters with individual $\sigma_x = 10\%$

**Error! Reference source not found.** 3 summarizes the results from the SRC sensitivity analysis method. The sign in front of the SRC indicates each element positive or negative influences. According to the table, primary suspension – longitudinal yaw stiffness ($K_{wx}$) appears to have the most substantial on increasing the critical speed. Bigoni *et al*. [6] indicated the same result, while Gao *et al*. [7] suggested the importance of the secondary lateral damper of a Chinese railway bogie. Global sensitivity analysis showed that the rear wheelset's stiffness is more significant than that of the front wheelset. Unfortunately, the primary suspension parameters are not considered variables in the work of Mehdi and Shaopu (1998) [4]. Of primary suspension parameters are $K_{wx}$ that have more impact than $K_{wy}$.

Table 3: SRC of each suspension parameter and conicity

| Parameter | $K_{wy}$ | $K_{wx}$ | $K_{ty}$ | $C_{ty}$ |
|---|---|---|---|---|
| SRC ($\beta_x$) | 0.06311 | 0.60140 | 0.01177 | 0.06703 |
| Parameter | $\lambda$ | | $K_{tx}$ | $C_{tx}$ |
| SRC ($\beta_x$) | - 0.76400 | | 0.03967 | 0.21501 |

The variation of $K_{tx}$ in the secondary suspension is insignificant to the system's dynamic behaviors. We found a strong influence of longitudinal dampers over the lateral damper in the secondary suspension system. The impact is also recognized by Mehdi and Shaopu [4]. The knowledge that the yaw dampers stabilize the vehicles is common to railway engineers. We enlist them as our significant parameters. However, the parameter is not considered essential [8] due to the selected probability distribution. The uncertainty is significant to both hybrid-global and global analysis. At different standard deviation values of 5%, 10%, and 20% on $K_{wx}$ alone, the calculated SRC increases with uncertainty. The SRC values of $K_{wx}$ are 0.3219, 0.60140, and 0.8213, respectively. More precise measurements can dramatically change the result. This concept allows maintenance engineers to mitigate the sensitive components' risk values by measuring their parameters more precisely and accurately.

In addition to the above analysis, we examine SRC of the equivalent conicity. Its highest value substantiates railway engineers' recognition of the limited value of the conicity when considering safety issues.

## IV. CONCLUSION

This study presents the effect of suspension parameters and conicity on the critical velocity for a linearized model of a two-axle bogie. The numerical method in solving the derived eigenvalue problem indicates that the velocity locates at the bifurcation point, beyond which lateral displacement of the vehicle rigorously oscillates until limited by flange contact forces. The hybrid-global sensitivity analysis using SRC is implemented to screen for the essential parameters. Specifying the significance of the parameter will assist involved engineers in improving the hunting behaviors of the vehicle. Longitudinal yaw stiffness of the primary suspension is critical to preventing excessive flange contact on a tangent track leading to flange wear and derailment. Other less important parameters are $K_{wy}$ of primary suspension and $K_{ty}$, $C_{ty}$, $K_{tx}$ , $C_{tx}$ of secondary suspension. In addition to suspension parameters, we found the most decisive influence of conicity on the value of critical velocity. These findings guided us to design suspension systems and rail systems better when the right-most attention was paid only to the essential parameters that matter to safety and maintenance issues.

## ACKNOWLEDGEMENT

This work (P1950662) is supported by Research Development Innovation Management for National Strategic and Network Division, National Science and Technology Development Agency, Thailand.

## REFERENCES

[1] *Railway applications - Testing and Simulation for the acceptance of running characteristics of railway vehicles - Running Behaviour and stationary tests*, EN 14363:2016, Mar. 2016.

[2] *Testing and Approval of Railway Vehicles from the Point of View of Their Dynamic Behaviour - Safety - Track Fatigue - Ride Quality*, UIC 518 (E), Sep. 2009.

[3] R. V. Dukkipati, S. Narayaswamy, and M. O. M. Osman, "Comparative performance of unconventional railway trucks," *Int. J. Vehicle Des*., vol. 19, no. 3, pp. 326–339, 1998.

[4] A. M. Whitman, "On the lateral stability of a flexible truck," *J. Dyn. Sys., Meas., Control*, vol. 105, no. 2, pp. 120–125, Jun. 1983, doi: 10.1115/1.3149642.

[5] A. M. Whitman and J. E. Molyneux, "Limit cycle behavior of a flexible truck," *J. Appl. Mech*., vol. 54, no. 4, pp. 930–934, Dec. 1987, doi: 10.1115/1.3173141.

[6] A. H. Wickens, "The dynamic stability of railway vehicle wheelsets and bogies having profiled wheels," *Int. J. Solids Struct.*, vol. 1, no. 3, pp. 319–341, 1965, doi: 10.1016/0020-7683(65)90037-5.

[7] A. H. Wickens, "Static and dynamic instabilities of bogie railway vehicles with linkage steered wheelset," *Vehicle Syst. Dyn.*, vol. 26, no. 1, pp. 1–16, 1996, doi: 10.1080/00423119608969299.

[8] R. V. Dukkipati and S. N. Swamy, "Lateral stability and steady state curving performance of unconventional rail trucks," *Mech. Mach. Theory*, vol. 36, no. 5, pp. 577–587, 2001, doi: 10.1016/S0094-114X(01)00006-4.

[9] D. Horak and D. N. Wormley, "Nonlinear stability and tracking of rail passenger truck," *J. Dyn. Sys., Meas., Control*, vol. 104, no. 3, pp. 256–263, 1982, doi: 10.1115/1.3139705.

[10] A. Mehdi and Y. Shaopu, "Effect of system nonlinearities on locomotive bogie hunting stability," *Vehicle Syst. Dyn*., vol. 29, no. 6, pp. 366–384, 1998, doi: 10.1080/00423119808969380.

[11] M. No and J. K. Hedrick, "High speed stability for rail vehicles considering varying conicity and creep coefficients," *Vehicle Syst. Dyn*., vol. 13, no. 6, pp. 299–313, 1984, doi: 10.1080/00423118408968780.

[12] J. Piotrowski, "Stability of freight vehicles with the H-frame 2-axle cross-braced bogies. Simplified theory," *Vehicle Syst. Dyn.*, vol. 17, no. 1-2, pp. 105–125, 1988, doi: 10.1080/00423118808968897.

[13] H. M. Sedighi and K. H. Shirazi, "Bifurcation analysis in hunting dynamical behavior in a railway bogie: Using novel exact equivalent functions for discontinuous nonlinearities," *Scientia Iranica*, vol. 19, no. 6, pp. 1493–1501, 2012, doi: 10.1016/j.scient.2012.10.028.

[14] V. K. Garg, and R. V. Dukkipat, *Dynamics of Railway Vehicle Systems*. Ontario, Canada: Academic Press, 1984.

[15] S.-Y. Lee and Y.-C. Cheng, "Hunting stability analysis of high-speed railway vehicle trucks on tangent tracks," *J. Sound Vib.*, vol. 282, no. 3-5, pp. 881–898, 2005, doi: https://doi.org/10.1016/j.jsv.2004.03.050.

[16] H. True, "Dynamics of a rolling wheelset," *Appl. Mech. Rev.*, vol. 46, no. 7, pp. 438–444, 1993, doi: 10.1115/1.3120372.

[17] N. K. Cooperrider, "The Hunting Behavior of Conventional Railway Trucks," *ASME J. Eng. Ind.*, vol. 94, no. 2, pp. 752–762, 1972, doi: 10.1115/1.3428240.

[18] J. S. Liu, *Monte Carlo strategies in scientific computing*, 2nd ed. New York, NY, USA: Springer, 2008.

[19] W. H. Press, S. A. Teukolsky, W. T. Vetterling, and B. P. Flannery, *Numerical Recipes in Fortran 77: The Art of Scientific Computing,* 2nd ed. Cambridge, U.K.: The Press Syndicate of the University of Cambridge, 2001.

[20] *Railway applications - Track - Rail - Part 1: Vignole railway rails 46 kg/m and above,* EN 13674-1:2011+A1:2017, May 2017.

[21] A. Saltelli, S. Tarantola, F. Campolongo, and M. Ratto, *Sensitivity Analysis in Practice: A Guide to Assessing Scientific Models*. West Sussex, U.K.: John Wiley & Sons, 2004.

[22] D. Bigoni, H. True, and A. P. Engsig-Karup, "Sensitivity analysis of the critical speed in railway vehicle dynamics," *Vehicle Syst. Dyn*., vol. 52, no. sup1, pp. 272–286, 2014, doi: 10.1080/00423114.2014.898776.

[23] X.-j. Gao, H. True, and Y.-h. Li, "Sensitivity analysis of the critical speed in a railway bogie system with uncertain parameters," *Vehicle Syst. Dyn.*, vol. 59, no. 2, pp. 224–244, 2021, doi: 10.1080/00423114.2019.1674.